

# Circulation Research

JOURNAL OF THE AMERICAN HEART ASSOCIATION



## Human Embryonic Stem Cells Develop Into Multiple Types of Cardiac Myocytes: Action Potential Characterization

Jia-Qiang He, Yue Ma, Youngsook Lee, James A. Thomson and Timothy J. Kamp  
*Circ. Res.* 2003;93:32-39; originally published online Jun 5, 2003;

DOI: 10.1161/01.RES.0000080317.92718.99

Circulation Research is published by the American Heart Association. 7272 Greenville Avenue, Dallas, TX 7514

Copyright © 2003 American Heart Association. All rights reserved. Print ISSN: 0009-7330. Online ISSN: 1524-4571

The online version of this article, along with updated information and services, is located on the World Wide Web at:

<http://circres.ahajournals.org/cgi/content/full/93/1/32>

Subscriptions: Information about subscribing to Circulation Research is online at  
<http://circres.ahajournals.org/subscriptions/>

Permissions: Permissions & Rights Desk, Lippincott Williams & Wilkins, a division of Wolters Kluwer Health, 351 West Camden Street, Baltimore, MD 21202-2436. Phone: 410-528-4050. Fax: 410-528-8550. E-mail: [journalpermissions@lww.com](mailto:journalpermissions@lww.com)

Reprints: Information about reprints can be found online at  
<http://www.lww.com/reprints>

## Human Embryonic Stem Cells Develop Into Multiple Types of Cardiac Myocytes Action Potential Characterization

Jia-Qiang He,\* Yue Ma,\* Youngsook Lee, James A. Thomson, Timothy J. Kamp

**Abstract**—Human embryonic stem (hES) cells can differentiate in vitro, forming embryoid bodies (EBs) composed of derivatives of all three embryonic germ layers. Spontaneously contracting outgrowths from these EBs contain cardiomyocytes (CMs); however, the types of human CMs and their functional properties are unknown. This study characterizes the contractions and action potentials (APs) from beating EB outgrowths cultured for 40 to 95 days. Spontaneous and electrical field-stimulated contractions were measured with video edge-detection microscopy.  $\beta$ -Adrenergic stimulation with 1.0  $\mu\text{mol/L}$  isoproterenol resulted in a significant increase in contraction magnitude. Intracellular electrical recordings using sharp KCl microelectrodes in beating EB outgrowths revealed three distinct classes of APs: nodal-like, embryonic atrial-like, and embryonic ventricular-like. The APs were described as embryonic based on the relatively depolarized resting membrane potential and slow AP upstroke. Repeated impalements of an individual beating outgrowth revealed a reproducible AP morphology recorded from different cells, suggesting that each outgrowth is composed of a predominant cell type. Complex functional properties typical of cardiac muscle were observed in the hES cell-derived CMs including rate adaptation of AP duration and provoked early and delayed afterdepolarizations. Repolarization of the AP showed a significant role for  $I_{\text{Kr}}$  based on E-4031 induced prolongation of AP duration as anticipated for human CMs. In conclusion, hES cells can differentiate into multiple types of CMs displaying functional properties characteristic of embryonic human cardiac muscle. Thus, hES provide a renewable source of distinct types of human cardiac myocytes for basic research, pharmacological testing, and potentially therapeutic applications. (*Circ Res*. 2003;93:32-39.)

**Key Words:** human embryonic stem cells ■ action potential ■ cellular electrophysiology ■ pharmacology  
■ cardiomyocytes

Recent studies have demonstrated that human embryonic stem (hES) cells in vitro can form embryoid bodies (EBs), some of which begin to spontaneously contract.<sup>1-3</sup> These beating EBs contain cardiac myocytes (CMs) based on the expression of cardiac-specific genes, cellular ultrastructure, and extracellular electrical activity.<sup>1,3</sup> Progress has been made in isolating cardiac myocytes from the mixed population of cells in the EB,<sup>2</sup> but no studies have yet defined what types of cardiac myocytes exist in the differentiating human EBs. In comparison, multiple types of mouse embryonic stem (mES) cell-derived CMs have been identified and characterized including nodal, atrial, ventricular, and Purkinje cells. However, mES cells have significant differences from hES cells such as variations in the stage-specific antigens and in the ability of leukemia inhibitory factor (LIF) to maintain the undifferentiated state.<sup>4</sup> Thus, differentiation of CMs from ES cells from the different species may be significantly different.

Defining the types of CMs that can be obtained from hES cells is essential for further research using this model system and for any potential utilization of these cells for cell-based therapies. A variety of techniques can be used to discriminate between different types of CMs including gene expression studies, immunochemistry, and perhaps most importantly, functional studies. The cardiac action potential (AP) is the result of multiple ion channels and  $\text{Ca}^{2+}$  cycling proteins interacting in concert, and so the AP provides a functional signature for the given type of CM.

The purpose of the present study is to characterize the contractions and APs in beating human EBs. These studies were performed in the intact EB outgrowths to avoid possible alterations produced by cell isolation or replating and culture of isolated cells. Because our focus was to determine if multiple types of cardiac myocytes can be obtained from hES cells, we chose to study a time window of 40 to 95 days of

Original received April 15, 2003; revision received May 23, 2003; accepted May 23, 2003.

From the Departments of Anatomy (Y.M., Y.L., J.A.T.), Medicine (T.J.K.), and Physiology (J.Q.H., T.J.K.), National Primate Research Center (Y.M., J.A.T.), University of Wisconsin, Madison, Wis.

\*Both authors contributed equally to this study.

Correspondence to Dr Timothy J. Kamp, University of Wisconsin-Madison, H6/343 Clinical Science Center, 600 Highland Ave, Madison, WI 53792-3248. E-mail: tjk@medicine.wisc.edu

© 2003 American Heart Association, Inc.

*Circulation Research* is available at <http://www.circresaha.org>

DOI: 10.1161/01.RES.0000080317.92718.99

differentiation of the EBs, which we predicted would provide adequate time for distinct cell types to become clear. The results begin to define the populations of hES cell-derived CMs and lay the groundwork for future investigation using defined populations of human CMs. A preliminary report of these findings has been presented.<sup>5</sup>

## Materials and Methods

### EB Formation and Cardiac Differentiation

The hES cell lines H1, H7, H9, and H14 were derived and maintained as previously described<sup>4</sup> and as per the expanded Materials and Methods section in the online data supplement available at <http://www.circresaha.org>. For EB formation, ES cell colonies were dispersed into cell aggregates containing approximately 500 to 800 cells using 1 mg/mL dispase. The cell aggregates were then cultured in suspension in cell culture flasks (BD Bioscience) with ES cell medium without basic fibroblast growth factor for 6 days with media changed daily. To promote cardiac differentiation, 6-day-old EBs were transferred to the 6 well plates coated with 0.1% gelatin in media consisting of DMEM supplemented with 15% FBS (selected for cardiac differentiation), 2 mmol/L L-glutamine, and 1% nonessential amino acids. During differentiation, the media was changed daily. Spontaneously contracting cells appeared as clusters in outgrowths from the EBs. These beating EBs were maintained in long-term cultures for up to 95 days.

### Immunostaining

Beating foci were isolated with Pasteur pipettes and digested with 0.05% trypsin for 20 minutes with intermittent vortexing. After cells were centrifuged and resuspended in DMEM containing 20% FCS and 0.5% chicken embryo extracts (GIBCO/BRL), cells were plated onto gelatin (0.3%)-coated coverslips, and incubated in 10% FCS medium for two days. Immunostaining was done as described elsewhere and in the online data supplement.<sup>6</sup>

### Contraction Measurements and Intracellular Electrophysiology

A single beating, microdissected EB outgrowth was cultured on a glass coverslip for 1 to 10 days, and the coverslip was then attached to the bottom of an experimental chamber mounted on an inverted microscope (Nikon Diaphot 200). The EBs were perfused with Tyrode's solution consisting of (in mmol/L) 140 NaCl, 5.4 KC1, 1 MgCl<sub>2</sub>, 10 HEPES, 10 glucose, 1.8 CaCl<sub>2</sub>, pH 7.4 with NaOH at 37°C. Contractions were measured using video edge detection as described in the online data supplement. For intracellular electrophysiology experiments, sharp glass microelectrodes were fabricated with resistances of 30 to 100 MΩ when filled with 3 mol/L KCl. Spontaneously beating EBs were impaled with the microelectrodes and electrode capacitance was nulled. Intracellular recordings of membrane potential were made using an Axoclamp-2A amplifier in Bridge Mode (Axon Instruments), and recordings that showed a stable maximum diastolic potential (MDP) for at least 5 minutes were included in data analysis. In some experiments, the preparation underwent electrical field stimulation at rates from 1 to 3 Hz. Data were digitized at 20 kHz and filtered at 2 kHz. APs were analyzed using pClamp 8.02 (Axon Instruments) and Origin 6.0 software (Microcal Inc) to determine AP duration at 50% and 90% of repolarization (APD50 and APD90), AP amplitude (APA), MDP, and the maximum rate of rise of the AP upstroke (dV/dt<sub>max</sub>). See the online data supplement for further details.

### Statistical Analysis

All values are presented as mean ± SD with n values representing the number of recordings in the data set. Statistical significance was evaluated by the Student's paired or unpaired *t* test (two-tail). One-way ANOVA followed by Newman Keuls test was used for multiple comparisons. Differences with *P* < 0.05 were considered statistically significant.

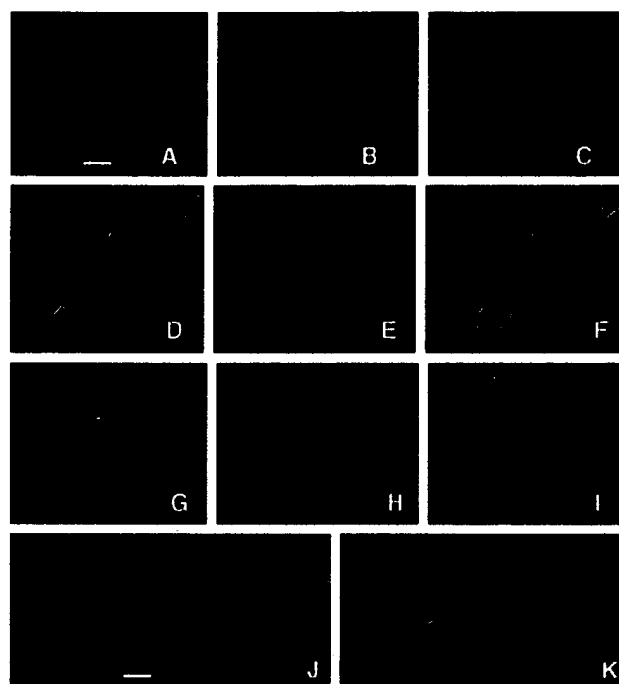


**Figure 1.** Expression of cardiac specific proteins. Cells isolated from beating outgrowths of human EBs were incubated with primary antibodies against  $\alpha$ -actinin (A), sarcomeric myosin heavy chain (D), and cardiac troponin I (G) followed by anti-mouse IgG coupled to Texas Red. All nuclei in the same field were stained with DAPI (B, E, and H). C, F, and I are double images of Texas Red and DAPI. Striated patterns of  $\alpha$ -actinin (J) and cTnI (K) are shown at a higher magnification. Scale bar in A indicates 20  $\mu$ m, and panels A to I are at the same magnification. Scale bar in panel J indicates 5  $\mu$ m, and panels J and K are at the same magnification.

## Results

### Cardiac Differentiation in EBs

Our initial studies showed that H1, H7, H9, and H14 ES cell lines can form EBs with spontaneously contracting outgrowths. Beating EBs are first observed approximately 10 days into differentiation and after 30 days approximately 10% to 25% of EBs show spontaneous contractions. With daily gentle media changes and low EB density, the EBs continued to contract in culture for a period of observation of up to 95 days of differentiation. The remainder of the experiments then focused on EBs derived from H9 and H14 cell lines, and results from these two cell lines were indistinguishable.

Immunostaining was performed to confirm the presence of CMs in the beating EB outgrowths and to examine contractile/sarcomeric protein organization (Figure 1). Beating foci were digested and plated as a monolayer for immunostaining using antibodies against  $\alpha$ -actinin, sarcomeric myosin heavy chain (MHC), and cardiac troponin I (cTnI). Cells isolated from beating foci resumed spontaneous beating after 6 to 48 hours plating on coverslips.

Staining with anti- $\alpha$ -actinin antibodies (Figure 1A) shows varying cytoplasmic patterns ranging from unorganized myofilaments to well-organized sarcomeric myofilaments with Z-lines (Figure 1J, at a higher magnification). Sarcomeric MHC staining shows an abundant signal distributed through-

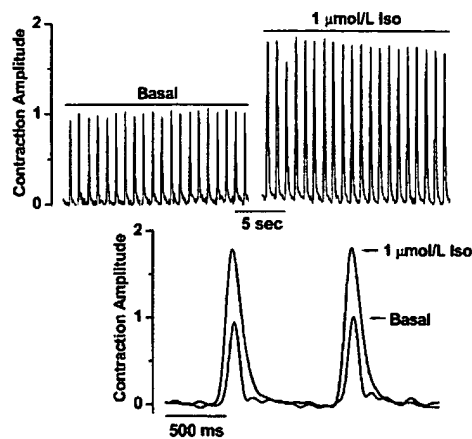


**Figure 2.** Effect on Iso on field-stimulated EB contraction. An EB is electrically field-stimulated at 1 Hz and contractions measured using video edge-detection techniques before and after application of  $1 \mu\text{mol/L}$  Iso.

out cytoplasm, which is a typical staining pattern with this antibody (Figure 1D).

Immunostaining of cTnI shows well-organized parallel myofilament (Figure 1G) and a striated pattern of I bands in some cells (Figure 1K, at a higher magnification). Nuclear staining of the same field are shown in Figures 1B, 1E, and 1H. These data clearly indicate that cardiac myocytes are present in differentiating EBs and some CMs show significant sarcomeric organization. Although cells were from beating foci, there are non-CMs indicated by nuclear staining but lack of cardiac-specific protein immunostaining. The percentage of CMs isolated from beating foci varied widely, ranging from 2% to 70%.

#### Positive Inotropic Response to $\beta$ -Adrenergic Stimulation

An increase in contractility of cardiac muscle in response to  $\beta$ -adrenergic stimulation requires appropriate surface mem-

brane receptors coupled to a signaling pathway that stimulates a variety of ion channels, membrane transporters, and myofilament proteins. However, the responsiveness of cardiac contractility to  $\beta$ -adrenergic stimulation changes over the course of development with the earliest embryonic cardiac myocytes being unresponsive to  $\beta$ -adrenergic agonists.<sup>7</sup> Therefore, we sought to determine if the beating EB outgrowths showed a change in contractile properties in response to the  $\beta$ -adrenergic agonist isoproterenol (Iso). Contractions of the EB outgrowths were measured using video edge-detection techniques during electrical field stimulation to control the beating rate. The magnitude of deflection of the edge of the outgrowth with each stimulated contraction gives a measure of contractility. Figure 2 demonstrates the contractile pattern of an EB stimulated at 1 Hz under basal conditions and then after superfusion with  $1 \mu\text{mol/L}$  Iso. A clear increase in the magnitude of the contraction is observed, and on average  $1 \mu\text{mol/L}$  Iso resulted in a  $33 \pm 27\%$  increase in the contraction magnitude ( $n=5, P=0.05$ ). This measurement showed significant variability from EB to EB (see the online data supplement for the full data set) in part due to the distinct and complex geometry of each beating outgrowth. These results demonstrate that  $\beta$ -adrenergic receptors are present in hES cell-derived CMs and stimulation of these receptors produce a positive inotropic response.

#### Patterns of Spontaneous Electrical Activity

Observations of beating EBs in culture revealed at least two distinct patterns of beating, continuous beating or episodic beating. To investigate this beating pattern further, we made intracellular recordings of APs with sharp microelectrodes in twenty spontaneously contracting EBs. Continuous electrical activity was documented in 12/20 EBs as shown by the example in Figure 3A. EBs with continuous electrical activity had spontaneous AP rates that were relatively constant throughout the recording period and ranged between 38 and

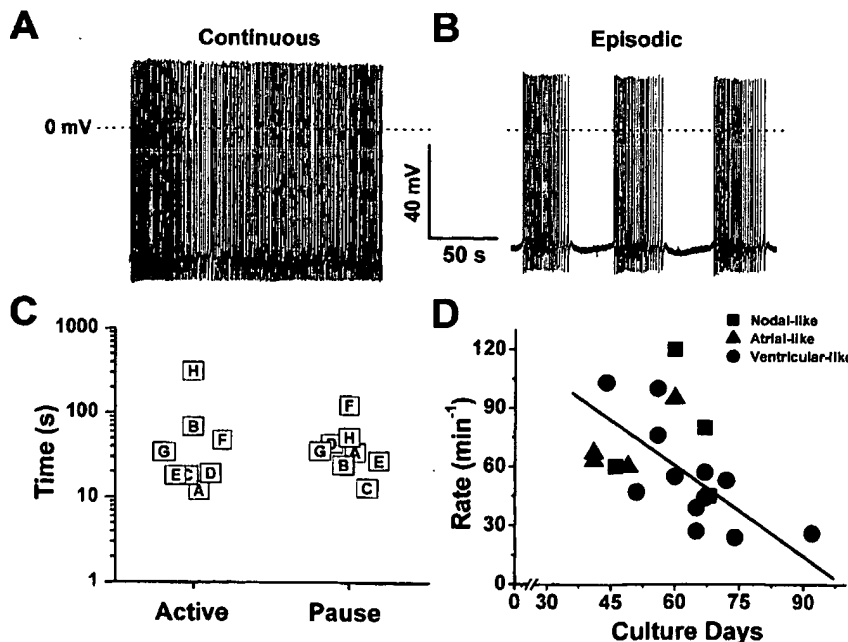


**Figure 3.** Electrical activity of spontaneous contracting human EBs. Intracellular APs were recorded by impaling sharp microelectrodes into beating EBs. Twelve of 20 EBs demonstrated a continuous activity (A) and 8 EBs showed episodic activity (B). For episodic EBs, the durations of the active periods and interspersed silent intervals are plotted for each EB with a letter denoting a given EB in C. In D, the rate of spontaneous activity for each EB studied as a function of days in culture is plotted. There was a general decrease in the spontaneous rate with time in culture for ventricular-like EBs. Linear regression  $R=-0.72, P<0.01$ .

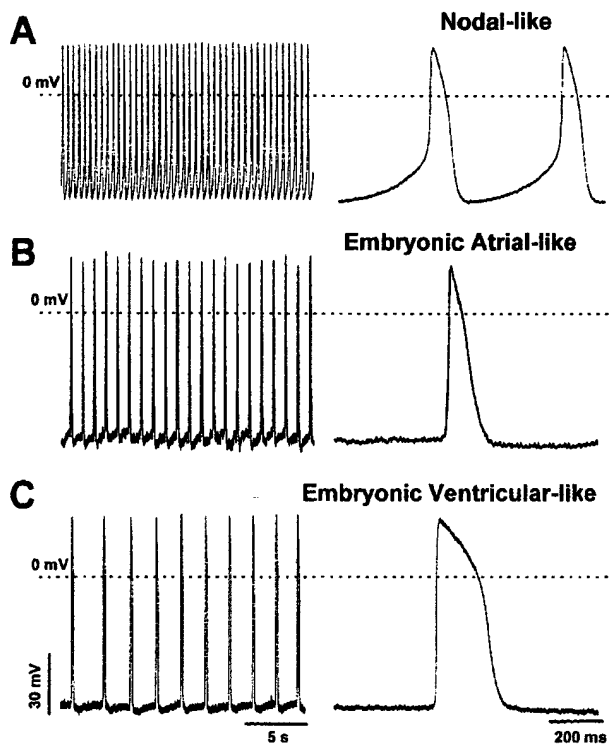


**Figure 4.** Multiple-type AP morphologies. Intracellular micro-electrode recordings from 3 different EB outgrowths demonstrating the 3 major types of APs observed: nodal-like (A), embryonic atrial-like (B), and embryonic ventricular-like (C).

106 bpm. In 8/20 EBs, episodic activity was observed, and a clear periodicity of activity was evident as shown in the example in Figure 3B. Each burst of activity is characterized by APs resuming at a relatively rapid rate that then tapers, followed by another pause. For episodic activity, the duration of active periods and pauses varied from EB to EB, and there was a rough parallel in the duration of spontaneous electrical activity and pauses for each EB (Figure 3C).

#### Multiple Types of APs

To characterize the types of CMs in the EBs, we examined the shape and properties of APs from 105 stable impalements of 20 different EBs. At the time window of differentiation that we studied (40 to 95 days), there was clear heterogeneity in the morphology of APs; however, APs could be classified into 3 major types: nodal-like, embryonic atrial-like, and embryonic ventricular-like (Figure 4). This classification was based on the properties of the AP as measured by the maximum rate of rise of the AP ( $dV/dt_{max}$ ), the AP duration

(APD), AP amplitude (APA), and prominence of phase 4 depolarization as summarized in the Table. Nodal-like APs (Figure 4A) were characterized by prominent phase-4 depolarization, slow upstroke ( $dV/dt_{max}$ ), and a smaller APA. Embryonic ventricular-like APs could be distinguished by the presence of a significant plateau phase of the AP resulting in a significantly longer duration compared with the more triangular shaped embryonic-atrial APs (see APD50 and APD90 comparisons in the Table). In addition, embryonic ventricular-like APs generally showed a trend for slower spontaneous rates of activity the longer the EBs were maintained in culture from 40 to 95 days (Figure 3D).

These latter two classes of APs are referred to as embryonic because they have properties more reminiscent of embryonic hearts, which are quite distinct from neonatal and adult cardiac muscle. In particular, the embryonic APs are characterized by more depolarized maximum diastolic potentials (MDP) and “slow” type APs based on low  $dV/dt_{max}$  ( $\approx 5$  to 30 V/sec).

To compare APs and hence cardiac cell types in a given EB outgrowth, we made multiple separate impalements with up to 14 separate recordings per outgrowth. Figure 5A demonstrates that multiple intracellular recordings from a single EB are characterized by a predominant AP phenotype. To provide a quantitative comparison of all of the APs recorded from each impalement of an EB, Figure 5B plots the measured APD90s grouped per EB. In general, the APD90s clustered closely together for a given EB but showed variability from EB to EB studied. These results suggest that for any given beating EB outgrowth, spontaneous differentiation favors a predominant cardiac myocyte cell type based on the reproducible AP morphology observed.

#### Rate Adaptation of APs

A fundamental property of cardiac myocytes is the ability to adapt to an increase in heart rate with a decrease in APD. Rate adaptation is present in atrial and ventricular muscle, and it can be impaired in certain disease states. Shortening of APD with rate has also been observed in embryonic (7 to 12 weeks) human ventricular muscle.<sup>8</sup> Therefore, we sought to determine if the embryonic ventricular-like APs exhibited appropriate rate adaptation. Isolated EB outgrowths were subjected to electrical field stimulation at three different rates, and steady state APs were then recorded and analyzed as shown in Figure 6. An increase in stimulation frequency from 1 to 2 Hz resulted in APD50 and APD90 shortening on average approximately 20% (Figure 6C), and there was an additional small decrease in APD as the rate was increased to 3 Hz. However, there were no changes in APA or upstroke of the

#### Characteristics of AP in hES Cell-Derived Beating EBs

	n (EB#)	Rate, bpm	APD50, ms	APD90, ms	$dV/dt_{max}$ , V/s	APA, mV	MDP, mV
Nodal-like	26 (5)	70.0 $\pm$ 23.2*	133.4 $\pm$ 20.7‡	168.6 $\pm$ 23.0‡	6.9 $\pm$ 3.1	68.5 $\pm$ 11.7‡	-49.2 $\pm$ 6.7†
Embryonic atrial-like	19 (5)	69.1 $\pm$ 23.6*	101.4 $\pm$ 24.8‡	131.1 $\pm$ 31.8‡	11.5 $\pm$ 4.2§	78.5 $\pm$ 9.4‡	-52.6 $\pm$ 8.3
Embryonic ventricular-like	60 (11)	47.1 $\pm$ 23.3	208.2 $\pm$ 60.3‡	247.2 $\pm$ 66.7‡	13.2 $\pm$ 6.2§	85.3 $\pm$ 9.3‡	-53.9 $\pm$ 8.6

Data are mean $\pm$ SD. n indicates the cell number; EB#, number of EBs; APD50/APD90, AP duration measured at 50% or 90% repolarization;  $dV/dt_{max}$ , maximum rate of rise of AP; APA, AP amplitude; and MDP, maximum diastolic potential.

\* $P$ <0.001 and † $P$ <0.01 compared with ventricular-like; ‡ $P$ <0.001 compared with each other; and § $P$ <0.001 compared with nodal-like.

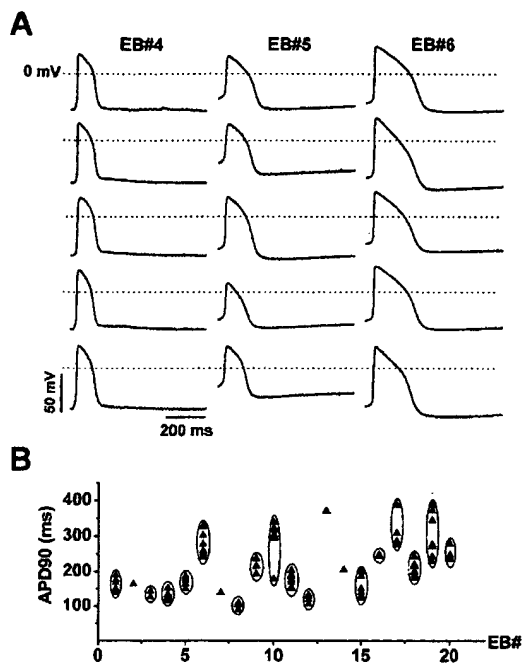


**Figure 5.** Each EB outgrowth characterized by a predominant AP morphology. **A**, Up to 14 repeated impalements of the same EB demonstrate reproducible AP morphologies as shown for 3 consecutive EBs studied by multiple impalements. EB#4 demonstrates embryonic atrial-like APs, EB#5 shows nodal-like APs, and EB#6 reveals embryonic ventricular-like APs. **B**, Plot of APD90 measured for each impalement in 20 consecutive EBs demonstrating clustering of APD in a given EB.

AP evident at the different stimulation rates tested. These results demonstrate that embryonic ventricular-like cardiac myocytes present in beating EBs have the necessary ion channels and regulatory properties to exhibit rate adaptation. Similar results were also observed for embryonic atrial-like myocytes (data not shown).

**hES Cell-Derived CMs Have Significant  $I_{Kr}$**   
Repopulation of the cardiac AP is due to multiple ionic currents with an important role played by voltage-gated  $K^+$

channels; however, there is significant species variability of the exact type of  $K^+$  channels present. In human heart, current through HERG potassium channels ( $KCNH_2$ ,  $I_{Kr}$ ) plays a major role in repolarization of the AP. HERG channels are also important in drug development as they represent a promiscuous target for drug block that can result in AP prolongation and the potentially lethal ventricular arrhythmias torsades de pointes.<sup>9</sup> Therefore, we examined the contribution of  $I_{Kr}$  to repolarization of APs in hES-derived CMs using the HERG-specific channel blocker E-4031. Application of 500 nmol/L E-4031 resulted in AP prolongation in both embryonic atrial and embryonic ventricular-like CMs (see Figures 7A and 7B). Prolongation of the AP was most evident for terminal repolarization (phase 3) where HERG current is maximal.<sup>10</sup> In embryonic atrial-like CMs, APD90 but not APD50 was significantly prolonged, and in embryonic ventricular-like CMs significant prolongation of both APD50 and APD90 was produced by E-4031 with a larger effect on APD90. There were not statistically significant effects by E-4031 on APA or MDP. These results suggest that HERG channels are expressed in both embryonic atrial-like and embryonic ventricular-like CMs and that  $I_{Kr}$  contributes significantly to repolarization of the APs in these cell types.

**Provoked Early and Delayed Afterdepolarizations**  
A major mechanism underlying certain types of cardiac arrhythmias is triggered activity, which results from afterdepolarizations. These can be divided into early afterdepolarizations (EADs), which occur during the repolarization of the AP, or delayed afterdepolarizations (DADs), which occur after full repolarization. EADs and DADs result from different cellular mechanisms, but both require a specific and complex set of interacting ion channels and  $Ca^{2+}$  cycling proteins present in cardiac myocytes. Therefore, we examined embryonic ventricular-like CMs for the ability to develop EADs and DADs. EADs typically occur in the setting of a prolonged AP. Figure 7C demonstrates an example of an EAD after treatment with E-4031. EADs were defined as

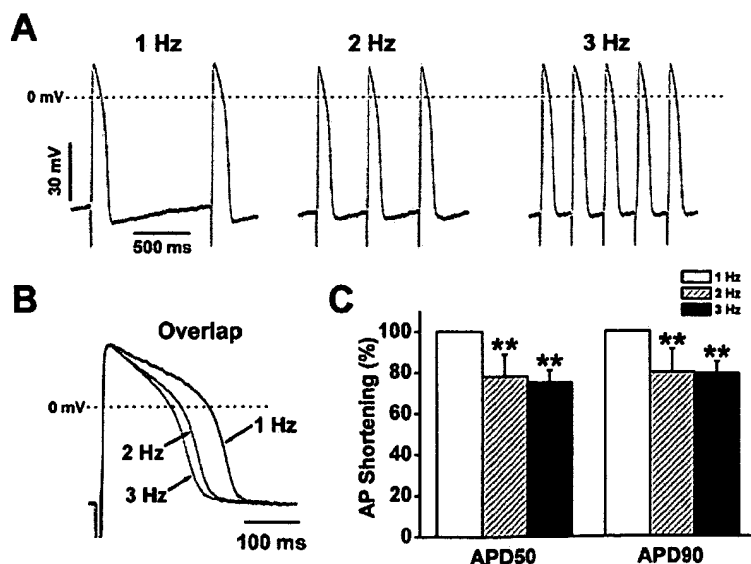


**Figure 6.** Rate adaptation of APs of hES cell-derived CMs. **A**, Field-stimulated embryonic ventricular-like APs were measured in an EB at 3 different stimulation rates: 1, 2, and 3 Hz. **B**, Overlapped APs at extended time scale with a clear decrease in APD with increasing frequency of stimulation. **C**, Average data for 4 to 7 experiments. \*\* $P<0.01$  compared with 1 Hz.

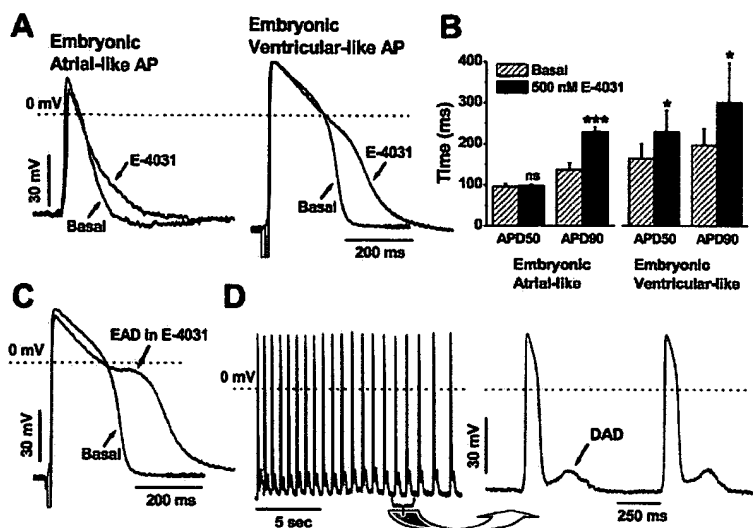


**Figure 7.** Effect of  $I_{K_r}$  block on APs and triggered activity. **A**, Representative overlapped embryonic atrial-like and ventricular-like APs before and after 500 nmol/L E-4031, a specific  $I_{K_r}$  blocker. **B**, Average data for APD50 and APD90 before and after 500 nmol/L E-4031 for 4 embryonic atrial-like CMs and 5 embryonic ventricular-like CMs. \* $P<0.05$  and \*\*\* $P<0.001$  compared with basal. **C**, Three of 5 embryonic ventricular-like recordings demonstrated EADs in the continued presence of E-4031. **D**, Spontaneous APs in an EB with associated DADs after each AP. Shortly after this recording, the cell progressively depolarized and became inactive, suggesting that this impalement damaged the cell.

depolarizations occurring near the AP plateau and were observed in 3/5 embryonic ventricular-like CMs treated with E-4031. EADs were never observed in the absence of E-4031. DADs typically occur during  $Ca^{2+}$  overload such as produced by injury or digoxin toxicity. Figure 7D shows an example of an EB recording with DADs after each AP. DADs were observed to occur spontaneously in a small number of cells immediately after microelectrode impalement presumably due to injury associated with impalement and associated  $Ca^{2+}$  overload. These cells were not used for characterization of AP properties, but they demonstrate the ability of the hES-derived CMs to exhibit DADs.

## Discussion

The results provide the first description of the functional heterogeneity of CMs obtained from hES cells using the EB system. AP analysis demonstrated the presence of nodal-like, embryonic atrial-like, and embryonic ventricular-like CMs. The CMs also exhibited the complex functional properties present in native cardiac myocytes including a positive inotropic response to  $\beta$ -adrenergic stimulation, AP rate adaptation, and the ability to exhibit afterdepolarizations. The finding of both functional atrial and ventricular-related cells agrees with previous RT-PCR detection of atrial and ventricular specific proteins, MLC2a and MLC2v in EBs.<sup>1</sup>

## AP Properties and Cardiomyogenesis

The development of the heart from precardiac mesoderm involves a complex series of cellular differentiation steps and morphogenetic changes that are reflected by changes in the electrical activity of the differentiating cardiac myocytes. Spontaneous electrical and mechanical activity is first observed in the developing heart after the formation of the linear heart tube or primary myocardium. Pacemaker type APs have been described using optical methods for the earliest contracting CMs in embryonic chick heart and rat heart.<sup>11</sup> The earliest microelectrode recordings were done on the 2-day chick embryo and revealed pacemaker-type APs characterized by a relatively depolarized MDP in the range of  $-35$  mV, prominent automaticity with a strong phase 4 depolarization, slow

$Ca^{2+}$ -dependent AP upstrokes, and small APA.<sup>12</sup> An in vitro model using mES cells was found to recapitulate this developmental stage as the earliest contracting cardiac myocytes found at 9 to 11 days of differentiation had homogenous pacemaker type APs.<sup>13</sup> L-type  $Ca^{2+}$  channels appear to be one of the earliest ion channels expressed in the CMs and play a critical role in the  $Ca^{2+}$ -dependent APs.<sup>14,15</sup> As cardiac differentiation proceeds, specialization of different types of cardiac myocytes beginning with the clear distinction between the atrial and ventricular chambers become evident. The resting membrane potential becomes progressively more negative in the developing atrial and ventricular myocytes, which correlates with an increasing presence of  $I_{K_1}$ .<sup>12,14</sup> In addition, there is a gradual appearance of a more rapid upstroke of the APs in both ventricular and atrial myocytes corresponding to an increasing density of  $I_{Na}$ .<sup>12,16</sup> Ultimately, the fetal atrial and ventricular myocytes exhibit stable resting membrane potentials approaching  $E_K$  with little automaticity and very rapid AP upstrokes. Similarly, the mouse EB system has identified intermediate stage CMs, which begin to show AP heterogeneity and exhibit intermediate MDPs and increasingly rapid AP upstrokes from days 12 to 15. This is followed on days 16 to 25 by terminal stage APs described as atrial-like, ventricular-like, and nodal-like.<sup>13,17</sup> Thus, there is an orderly progression of ion channel expression and AP morphologies during the course of heart development that has been recapitulated in the murine EB system.

The present study using hES cells examined EBs maintained in culture 40 to 95 days and found heterogeneity of AP morphologies. Although APs with characteristics of atrial and ventricular myocytes were observed, the relatively positive MDP ( $-50$  to  $-60$  mV) and the slow AP upstroke (5 to 30 V/sec) contrasts with neonatal and adult human atrial and ventricular CMs, which have resting membrane potentials in the range of  $-80$  mV and  $dV/dt_{max}$  ranging from 150 to 350 V/s.<sup>18</sup> The hES cell-derived CMs likely correlate with the "intermediate" stage described for the mES cell system.<sup>13,19</sup> The limited data available describing the AP in human embryonic and fetal hearts suggests that by 7 to 8 weeks of development the resting membrane potential and  $dV/dt_{max}$  of

atrial and ventricular myocytes reaches that of adult cells.<sup>8,20</sup> Thus, we referred to the atrial and ventricular APs observed in this study as embryonic because they have properties of APs anticipated in human embryos before 7 weeks of development. The nodal type APs observed were simply described as nodal because this AP morphology shows little change during development. This strikingly slow in vitro development of AP properties compared with the mouse system is likely related to the markedly different gestational periods comparing mice and man.

The adult human heart contains a much greater heterogeneity of distinct functional types of cardiomyocytes than the human EB model observed to date. For example, there is heterogeneity in atrial AP morphology in different regions of the atria,<sup>18</sup> and likewise there is a well-described transmural heterogeneity of the ventricular AP.<sup>21</sup> Multiple specialized cell populations exist in the sinoatrial and atrioventricular nodes that all have their own signature APs.<sup>22</sup> Potentially, some approaches in the in vitro EB differentiation model will be able to favor development of more mature and specialized cells. For example, in mouse EBs, treatment with endothelin-1 favors differentiation of Purkinje type CMs.<sup>23</sup>

### EB Outgrowth Composition

It has been assumed that because enzymatic dissociation of a collection of EB outgrowths has yielded diverse CM cell types, that each outgrowth is composed of a heterogeneous mix of CMs perhaps in part mimicking the heterogeneous collection of myocytes in the developing heart.<sup>19</sup> However, the current intracellular recording of APs with sharp micro-electrodes were unique in that repeated distinct cellular measurements were made from individual outgrowths, and we found that each outgrowth is populated by a predominant cell type. This finding was also suggested in more recent studies using the ventricular-specific MLC2V promoter to drive the expression of GFP in mouse EBs.<sup>24</sup> Thus, we postulate that each outgrowth responds to its unique micro-environment resulting in differentiation and proliferation of one predominant type of CM.

Despite our finding of a predominant AP morphology in the EB outgrowth, these structures are complex and do not contain an absolutely uniform population of cardiac myocytes. Extracellular electrical mapping studies using multi-electrode arrays of beating human EB outgrowths have previously demonstrated that the CMs form a functional electrical syncytium connected by gap junctions, which typically have a stable focal origin for activation.<sup>3</sup> Examination of the majority of the intracellular APs made in this study confirms the suggestion that excitation spreads rapidly from adjacent cells based on the minimal phase 4 depolarization measured followed by the sudden upstroke of the AP, saltatory conduction. Thus, some areas of the outgrowth exhibit greater automaticity and behave as the pacemaker for the outgrowth. This could be due to the presence of a distinct cell type or just an extreme of the predominant cell type of the EB, such as an embryonic ventricular-like cell with a more rapid phase 4 depolarization. Future efforts will be needed to better define the cellular composition of individual out-

growths and define the factors that favor differentiation to particular CM cell lineages.

### Spontaneous Electrical Activity Patterns

Distinct beating patterns observed in the EB outgrowths suggest further functional and structural complexity of the EBs. In the simplest case, a regular pattern of spontaneous electrical activity was likely due to regular activation emanating from a focal pacemaker and spreading throughout the electrically coupled CMs as observed in a previous study making extracellular recordings with multielectrode arrays.<sup>3</sup> However, some EBs display a more complex rhythmicity with episodic beating as has been observed in the mouse EB system using multielectrode array mapping studies.<sup>25</sup> In that mouse EB study, intermittent failure of AP propagation was clearly documented and was concluded to be due to impedance mismatch from structural discontinuities in the network of interconnected CMs. Studies using 2-dimensional culture systems of neonatal myocytes have also pointed to the importance of tissue geometry and branching to produce current-load mismatches that can slow conduction and produce conduction blocks.<sup>26</sup> Other mechanisms can also contribute to the failure of AP propagation such as impaired cell-to-cell coupling (gap junctions) and reduced cellular excitability (upstroke of AP).<sup>27-29</sup> The complex pattern of impulse propagation seen in these episodically beating EBs provides a potential model for understanding areas of localized slow conduction present in the intact heart, such as the AV node,<sup>30</sup> and also for pathological conditions such as reentrant arrhythmias or certain forms of heart block.

### Future Implications and Uses of hES Cells

Efforts at further defining and isolating the distinct CM cell populations will be an important focus of future research and may use genetic selection strategies that have proved effective for mES cells.<sup>24,31,32</sup> A major challenge will be to produce more specialized and mature hES cell-derived CMs. Nevertheless, the present system provides an in vitro model for human cardiac development and basic research studies. This system may also provide a model for heart failure as CMs from failing hearts typically revert to a more fetal or embryonic gene expression pattern. Ultimately, the hES cell model allows research studies focusing on human-specific proteins and functional properties. For example,  $I_{Kr}$  is found at very low levels in mouse CMs, whereas it provides a major current for repolarization of the human heart and hES cell-derived CMs. Finally, given the ability of hES cells to differentiate into cardiomyocytes, there is long-term promise for hES cells in cell-based therapies for heart disease.

### Acknowledgments

This work was supported by NIH grants PO1 HL47053 (T.J.K.), R21 HL72089 (T.J.K., J.A.T.), R01 HL67050 (Y.L.), a grant from the University of Wisconsin Cardiovascular Research Center (T.J.K., J.A.T.), and the WiCell Research Institute, a nonprofit subsidiary of the Wisconsin Alumni Research Foundation. Human ES cells are made available to research by the WiCell Research Institute to academic/nonprofit researchers on a cost-recovery basis under the terms of a Memorandum of Understanding and Simple Letter Agreement. We gratefully acknowledge the invaluable suggestions from Dr Craig T. January.

## References

1. Kehat I, Kenyagin-Karsenti D, Snir M, Segev H, Amit M, Gepstein A, Livne E, Binah O, Itskovitz-Eldor J, Gepstein L. Human embryonic stem cells can differentiate into myocytes with structural and functional properties of cardiomyocytes. *J Clin Invest.* 2001;108:407–414.
2. Xu C, Police S, Rao N, Carpenter MK. Characterization and enrichment of cardiomyocytes derived from human embryonic stem cells. *Circ Res.* 2002;91:501–508.
3. Kehat I, Gepstein A, Spira A, Itskovitz-Eldor J, Gepstein L. High-resolution electrophysiological assessment of human embryonic stem cell-derived cardiomyocytes: a novel in vitro model for the study of conduction. *Circ Res.* 2002;91:659–661.
4. Thomson JA, Itskovitz-Eldor J, Shapiro SS, Waknitz MA, Swiergiel JJ, Marshall VS, Jones JM. Embryonic stem cell lines derived from human blastocysts. *Science.* 1998;282:1145–1147.
5. He J-Q, Ma Y, Causey J, Lee Y, Thomson JA, Kamp TJ. Human embryonic stem cell-derived embryoid bodies exhibit multiple types of cardiac action potentials. *Biophys J.* 2003;84:33a. Abstract.
6. Yu YT, Breitbarth RE, Smoot LB, Lee Y, Mahdavi V, Nadal-Ginard B. Human myocyte-specific enhancer factor 2 comprises a group of tissue-restricted MADS box transcription factors. *Genes Dev.* 1992;6:1783–1798.
7. Chen FM, Yamamura HI, Roeske WR. Ontogeny of mammalian myocardial  $\beta$ -adrenergic receptors. *Eur J Pharmacol.* 1979;58:255–264.
8. Jezek K, Pucelik P, Sauer J, Bartak F. Basic electrophysiological parameters and frequency sensitivity of the ventricular myocardium of human embryos. *Physiol Bohemoslov.* 1982;31:11–19.
9. Vorperian VR, Zhou Z, Mohammad S, Hoon TJ, Studenik C, January CT. Torsade de pointes with an antihistamine metabolite: potassium channel blockade with desmethylastemizole. *J Am Coll Cardiol.* 1996;28:1556–1561.
10. Zhou Z, Gong Q, Ye B, Fan Z, Makielski JC, Robertson GA, January CT. Properties of HERG channels stably expressed in HEK 293 cells studied at physiological temperature. *Biophys J.* 1998;74:230–241.
11. Kamino K. Optical approaches to ontogeny of electrical activity and related functional organization during early heart development. *Physiol Rev.* 1991;71:53–91.
12. Sperelakis N, Shigenobu K. Changes in membrane properties of chick embryonic hearts during development. *J Gen Physiol.* 1972;60:430–453.
13. Maltsev VA, Rohwedel J, Hescheler J, Wobus AM. Embryonic stem cells differentiate in vitro into cardiomyocytes representing sinus nodal, atrial and ventricular cell types. *Mech Dev.* 1993;44:41–50.
14. Maltsev VA, Wobus AM, Rohwedel J, Bader M, Hescheler J. Cardiomyocytes differentiated in vitro from embryonic stem cells developmentally express cardiac-specific genes and ionic currents. *Circ Res.* 1994;75:233–244.
15. Kolossov E, Fleischmann BK, Liu Q, Bloch W, Viatchenko-Karpinski S, Manzke O, Ji GJ, Bohnen H, Addicks K, Hescheler J. Functional characteristics of ES cell-derived cardiac precursor cells identified by tissue-specific expression of the green fluorescent protein. *J Cell Biol.* 1998;143:2045–2056.
16. Pappano AJ. Action potentials in chick atria: increased susceptibility to blockade by tetrodotoxin during embryonic development. *Circ Res.* 1972;31:379–388.
17. Zhang YM, Hartzell C, Narlow M, Dudley SC Jr. Stem cell-derived cardiomyocytes demonstrate arrhythmic potential. *Circ Res.* 2002;106:1294–1299.
18. Schram G, Pourrier M, Melnyk P, Nattel S. Differential distribution of cardiac ion channel expression as a basis for regional specialization in electrical function. *Circ Res.* 2002;90:939–950.
19. Hescheler J, Fleischmann BK, Lentini S, Maltsev VA, Rohwedel J, Wobus AM, Addicks K. Embryonic stem cells: a model to study structural and functional properties in cardiomyogenesis. *Cardiovasc Res.* 1997;36:149–162.
20. Tuganowski W, Tendera M. Components of the action potential of human embryonic auricle. *Am J Physiol.* 1973;224:803–808.
21. Antzelevitch C, Sicouri S, Litovsky SH, Lukas A, Krishnan SC, Di Diego JM, Gintant GA, Liu D-A. Heterogeneity within the ventricular wall: electrophysiology and pharmacology of epicardial, endocardial, and M cells. *Circ Res.* 1991;69:1427–1449.
22. Efimov IR, Mazgalev TN. High-resolution, three-dimensional fluorescent imaging reveals multilayer conduction pattern in the atrioventricular node. *Circ Res.* 1998;98:54–57.
23. Gourdie RG, Wei Y, Kim D, Klatt SC, Mikawa T. Endothelin-induced conversion of embryonic heart muscle cells into impulse-conducting Purkinje fibers. *Proc Natl Acad Sci U S A.* 1998;95:6815–6818.
24. Muller M, Fleischmann BK, Selbert S, Ji GJ, Endl E, Middeler G, Muller OJ, Schlenke P, Frese S, Wobus AM, Hescheler J, Katus HA, Franz WM. Selection of ventricular-like cardiomyocytes from ES cells in vitro. *FASEB J.* 2000;14:2540–2548.
25. Igelmund P, Fleischmann BK, Fischer IR, Soest J, Gryshchenko O, Bohm-Pinger MM, Sauer H, Liu Q, Hescheler J. Action potential propagation failures in long-term recordings from embryonic stem cell-derived cardiomyocytes in tissue culture. *Pflugers Arch.* 1999;437:669–679.
26. Kucera JP, Kleber AG, Rohr S. Slow conduction in cardiac tissue, II: effects of branching tissue geometry. *Circ Res.* 1998;83:795–805.
27. Dominguez G, Fozard HA. Influence of extracellular K<sup>+</sup> concentration on cable properties and excitability of sheep cardiac Purkinje fibers. *Circ Res.* 1970;26:565–574.
28. Rohr S, Kucera JP, Kleber AG. Slow conduction in cardiac tissue, I: effects of a reduction of excitability versus a reduction of electrical coupling on microconduction. *Circ Res.* 1998;83:781–794.
29. Delmar M, Michaels DC, Johnson T, Jalife J. Effects of increasing intercellular resistance on transverse and longitudinal propagation in sheep epicardial muscle. *Circ Res.* 1987;60:780–785.
30. Meijler FL, Janse MJ. Morphology and electrophysiology of the mammalian atrioventricular node. *Physiol Rev.* 1988;68:608–647.
31. Klug MG, Soopas MH, Koh GY, Field LJ. Genetically selected cardiomyocytes from differentiating embryonic stem cells form stable intracardiac grafts. *J Clin Invest.* 1996;98:216–224.
32. Meyer N, Jaconi M, Landopoulou A, Fort P, Puceat M. A fluorescent reporter gene as a marker for ventricular specification in ES-derived cardiac cells. *FEBS Lett.* 2000;478:151–158.